The role of beach state and the timing of pre-storm surveys in determining the accuracy of storm impact assessments

Jessamin A. Straub[a], Antonio B. Rodriguez[a,*], Richard A. Luettich[a], Laura J. Moore[b], Michael Itzkin[b], Justin T. Ridge[c], Alexander C. Seymour[c], David W. Johnston[c], Ethan J. Theuerkauf[d]

[a] University of North Carolina at Chapel Hill, Institute of Marine Sciences, Morehead City, NC 28557, USA
[b] University of North Carolina at Chapel Hill, Department of Geological Sciences, Chapel Hill, NC 27599, USA
[c] Division of Marine Science and Conservation, Nicholas School of the Environment, Duke University Marine Laboratory, Beaufort, NC 28516, USA
[d] Michigan State University, Department of Geography, Environment, and Spatial Sciences East Lansing, MI 48824, USA

ARTICLE INFO

Editor: Shu Gao

Keywords:
Beach
Coastal hazard
Storm impact
Swash
Collision
Overwash

ABSTRACT

Dune erosion principally occurs when water level exceeds the elevation of the beach and predicting erosion is progressively becoming more important for management as coastal populations increase, sea level rises, and storms become more powerful. This study assesses storm impacts using a simple model from Stockdon et al. (2007) configured with oceanographic information from the ADCIRC + SWAN model and frequently collected beach profiles. We applied that model to barrier islands in North Carolina including: Core Banks with a more dissipative beach morphology and Shackleford Banks and Onslow Beach with intermediate beach morphologies. The study periods captured 10 events where wave collision with the dunes and/or overwash were either predicted or observed, including large multiple-day events caused by hurricanes and smaller events caused by onshore winds and high tide. Comparing model output with a time series of beach photographs shows the predictive power and sensitivity of the model was consistently high at the Core Banks Site with its wide and low-gradient beach, high-elevation dunes (2.58 m), and high resistance to overwash. Model predictive power and sensitivity was lowest at the Shackleford Banks Site because frequent and large changes to beach slope and intermediate dune elevation (0.54–1.25 m) caused small variations of modeled total water level to either overpredict or underpredict storm impacts. In addition, storm impacts were always overpredicted during hurricanes at the Shackleford Banks Site, which was likely due to storm waves decreasing the beach slope from what was measured prior to the event and used as model input. Like Shackleford Banks, the beach slope of the Onslow Beach Site was steep and variable, but the low-elevation dunes (0.24–0.28 m) made resistance to overwash low and the predictive power and sensitivity of the model higher than at the Shackleford Banks Site. Results suggest that storm impacts and the associated potential for dune erosion is predicted more accurately at beaches where the threshold for overwash is high or low because total water level during most events will commonly fall short of or exceed the overwash threshold, respectively. The accuracy of predicting the storm impact regime is sensitive to beach slope. The slope of intermediate beaches is more variable than dissipative beaches and requires frequent measurement if it is to be represented accurately in the model, but this can be impractical and costly even using the latest drone-surveying methods. To maximize the accuracy of predicting storm impacts, intermediate beach morphology should be constrained by surveying at seasonal or yearly time scales and used as input to numerical models that estimate beach slope over short time scales (hours during an event or daily), configured with the latest wave and water-level forecasts.

1. Introduction

Coastal hazards such as erosion and flooding, expose communities to risk including loss of property, infrastructure, and habitats, in addition to the associated societal damages resulting from loss of personal income, displacement of families, and an increase in accidental deaths. To better inform assessments of risk exposure, researchers are striving to improve understanding of how physical processes and

* Corresponding author.
E-mail address: abrodrig@email.unc.edu (A.B. Rodriguez).

https://doi.org/10.1016/j.margeo.2020.106201
Received 17 December 2019; Received in revised form 4 April 2020; Accepted 11 April 2020
Available online 14 April 2020

associated timescales drive coastal morphologic change during storms (e.g., Ruggiero et al., 2001; Morton, 2002; Burroughs and Tebbens, 2008; Stockdon et al., 2013; Long et al., 2014). The vulnerability of coastal communities to storms is defined, in part, by the characteristics of the storm (e.g. strength, duration, and trajectory), the morphology of the coastline (e.g. beach slope, dune elevation, and dune width), and the timescales over which morphologic changes occur (e.g. frequency of erosion events vs. duration of morphologic recovery; Sallenger, 2000).

Along coastal barrier islands, dunes commonly separate the beach from the built environment and their relatively high elevation protects communities by providing a natural barrier from waves and high-water during storms. Coastal-foredune morphology is dynamic along some beaches, subject to wave and current erosion when water levels are high, and accretion when wind transports sand along and across the shoreline. Forecasting coastal-dune erosion is challenging due to the complex interactions between sediment transport, beach morphology, vegetation, and fluid dynamics (e.g., Short and Hesp, 1982; Hesp, 1988; Hesp, 2002; Psuty, 2008; Durán and Moore, 2013; Ranasinghe, 2016). Accurately predicting when ocean-water level reaches the base of the dunes and is therefore capable of causing erosion, is necessary to assess the vulnerability of communities to flooding, and support management practices aimed at increasing resilience (Sallenger, 2000; Roelvink et al., 2009; Long et al., 2014).

The severity and type of storm impact along sandy coastlines is commonly characterized using the storm impact scale presented by Sallenger (2000), which defines (from lowest to highest impact) swash, collision, overwash, and inundation regimes. Regimes are identified by the elevation of high and low extremes of swash (R_{high} and R_{low}) determined by the tide, storm surge, and wave runup levels relative to the elevation of the coastal dune toe and crest. During the swash, collision, and overwash regimes, R_{high} is positioned below the dune toe, between the dune toe and the dune crest, and above the dune crest, respectively. During the inundation regime the beach and dunes become completely submerged by storm-induced high-water levels (Sallenger, 2000).

Storm-impact assessments apply the relationships from the storm impact scale using recent metrics of dune morphology (beach slope, dune crest, and dune toe elevations), in combination with storm hydrodynamics, to predict the likelihood of different impact regimes (e.g. Ruggiero et al., 2001; Stockdon et al., 2006, 2007; Roelvink et al., 2009). The accuracy of storm-impact assessments is sensitive to the accuracy of the measurements and predictions on which they are based. Ideally, measurements of beach and dune morphology are collected immediately prior to a storm, but given the challenges associated with high-frequency data collection and surveying as a storm approaches (safety concerns, and/or resource constraints) this isn't always possible (Casella et al., 2014; Klemas, 2015; Seymour et al., 2018). To assess morphology, researchers mainly rely on aerial LiDAR surveys (Stockdon et al., 2002; Sallenger Jr. et al., 2003; Le Mauff et al., 2018), but surveys are not always conducted during the same season as a storm event, and therefore may not accurately represent the beach and dune morphology present at the start of a storm. This mismatch between the timing of data collection and storm occurrence will likely influence the accuracy of storm impact regime predictions (Morton, 2002; Doran et al., 2015). We hypothesize that in the case of such a mismatch, the accuracy of storm impact assessments will be a function of the degree to which a beach tends to be in a more reflective vs. dissipative state because the beach morphology of the former tends to be more dynamic, making the capture of up-to-date dune elevations and beach slopes more challenging.

Storm impact regimes have been shown to vary alongshore during large storm events as beach morphology transitions between dissipative and more reflective states (Sallenger, 2000; Stockdon et al., 2007; Long et al., 2014), but there is a need for studies that examine the effect of beach state on the accuracy of storm impact assessment over longer time scales (multiple months). This study is aimed at evaluating the predictive skill of the Stockdon et al. (2007) model for predicting storm impact regimes at three barrier island sites. We test whether prediction accuracy decreases from dissipative to intermediate beaches as the actual dune elevations and beach slopes deviate over time from that which was measured. Supplementing previous studies that focus on predicting storm impact regimes at the event temporal scale and large (> 1 km) spatial scales (e.g. Stockdon et al., 2007; Long et al., 2014), we focus on predicting the storm impact regimes of collision and overwash (because inundation was limited) at individual barrier-island profiles continuously over multiple-month periods, and comparing prediction accuracy across different beach slopes and different degrees of elapsed time between pre-storm survey and storm occurrence.

1.1. Study sites

We selected the central North Carolina coast for this study because within proximity (75 km) there exist barrier islands with distinct orientations, beach and dune morphologies, and wave climates. The sites are on undeveloped wave-dominated barrier islands with a mean tidal range of ~0.95 m, including east-facing south Core Banks (Cape Hatteras National Seashore), southwest-facing east Shackleford Banks (Cape Hatteras National Seashore), and southeast-facing Onslow Beach (Marine Corps Base Camp Lejeune; Fig. 1).

Core Banks is a high-energy barrier island representative of a dissipative beach (Short and Hesp, 1982; Dolan and Lins, 1985; Riggs and Ames, 2007). The site is characterized by a gentle beach slope (~0.01–0.04), a wide backshore and foreshore (~60 m total), and high dunes (~4 m). From 1946 to 2009 the Core Banks Site had an average ocean-facing shoreline erosion rate of 0.64 m/yr (http://ncdenr.maps.arcgis.com). The beach site at Shackleford Banks is located adjacent to Cape Lookout Bight, an embayment that formed in the 1960s through anthropogenically-induced spit migration to the north-northwest (Wells, 1988; Elliott et al., 2015). The spit extends to within 1.5 km south of the site and refracts ocean waves. The site is characterized by a steep beach slope (~0.04–0.1), a narrow foreshore extending to the dune toe (~16 m), and ~3 m-high dunes, representing an intermediate beach (Susman and Heron Jr, 1979; Short and Hesp, 1982). Shackleford Banks is one of only a few barrier islands along the U.S. East Coast that faces south and, compared to Core Banks, is less affected by extratropical storms (nor'easters), has less intense wave energies overall (Heron Jr et al., 1984), and yet our site experienced average shoreline erosion of 1.62 m/yr from 1946 to 2009 (http://ncdenr.maps.arcgis.com; Division of Coastal Management Oceanfront Erosion Rates 2013). Onslow Beach is separated from the mainland by saltmarsh and the Intracoastal Waterway located between the New River Inlet to the southwest and Brown's Inlet to the northeast. The Onslow Beach site is an intermediate beach with a wide range of beach slopes (~0.01–0.1), and low-elevation (~1.50 m) dunes (Short and Hesp, 1982; Rodriguez et al., 2012; Theuerkauf and Rodriguez, 2014). From 1952 to 2009 the Onslow Beach Site had an average shoreline erosion rate of 3.41 m/yr (http://ncdenr.maps.arcgis.com; Division of Coastal Management Oceanfront Erosion Rates 2013) and experienced frequent overwash and washover deposition since Hurricane Irene impacted the area in August 2011 (Theuerkauf and Rodriguez, 2014; VanDusen et al., 2016).

2. Methods

2.1. Field data collection

2.1.1. Camera traps and water-level loggers

To document the storm impact regimes at the sites, we collected photos and water-level data at Core Banks and Shackleford Banks from August 2017–March 2018 and at Onslow Beach from June 2012–December 2014. The first four months of Onslow Beach data are from VanDusen et al. (2016). The photographs were used to identify collision and overwash events. The logger data helped to determine the proximity of the ocean-water elevation to the base of the dune, which is

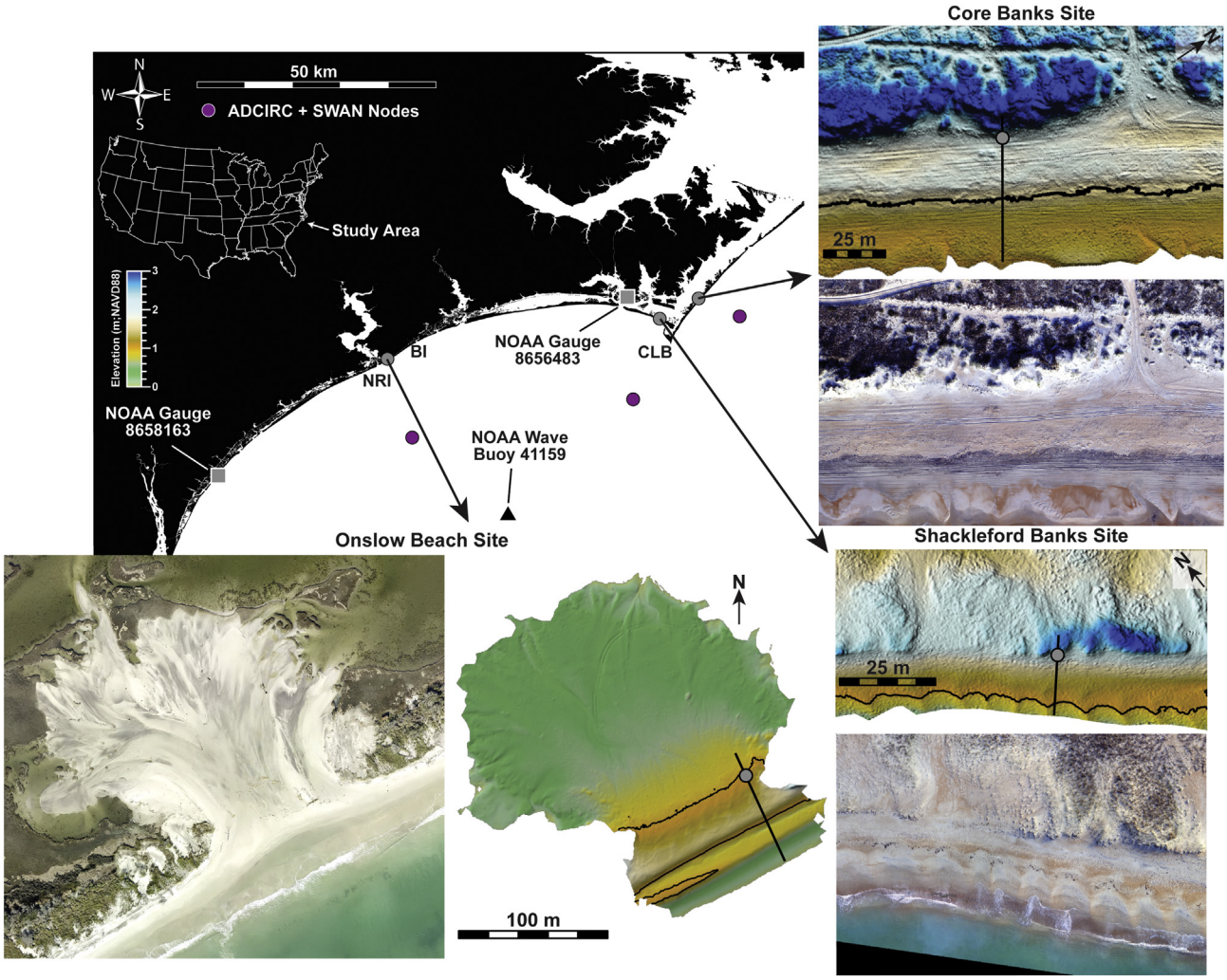

Fig. 1. Location map of the study sites in North Carolina, including: Core Banks, Shackleford Banks, and Onslow Beach. Example DEMs of each site are at the same vertical scale and show locations of beach transects (black lines) and water-level loggers suspended in shallow wells (gray circles). The 1.0 m contour is shown for Onslow Beach and Shackleford Banks and the 1.5 m contour for Core Banks in black. Camera traps were installed within 20 m of the wells on the dunes and oriented with their field of view aimed along the beach, capturing the wells in each photo. The location of the NOAA water-level gauges (gray squares) and a wave buoy (black triangle) used in this analysis are also shown. CLB = Cape Lookout Bight; BI = Browns Inlet; NRI = New River Inlet.

the threshold between swash and collision. We deployed Reconyx Hyperfire HC500 trail cameras mounted to fence poles installed on the dune crest and oriented along the dune line facing the base of the dunes (system illustrated in VanDusen et al., 2016). Each camera was programmed to take a picture every 5 min during daylight hours (0700–1900 EST). Collision and overwash events were identified by inspecting the beach photos. The duration of impact regimes above swash was defined as extending from the first day collision and/or overwash was observed or predicted, to when the impact regime returned to swash.

At Core and Shackleford Banks, shallow wells with HOBO water level loggers suspended inside were installed seaward of the dune toe and at Onslow Beach landward of the dune crest (VanDusen et al., 2016). The logger was placed landward of the dune crest at Onslow Beach to mitigate equipment loss because this site has high shoreline-erosion rates. The water-level logger recorded data continuously every 5 min at Core Banks and Shackleford Banks, while the sampling frequency at Onslow Beach was set to 2-minute intervals. Sampling frequency was chosen based on digital storage space and site accessibility. The lower sampling frequency at Core and Shackleford banks was due to the sites only being accessible by boat, allowing for less frequent data downloads. During logger deployment and when data were downloaded, elevation measurements were collected on the ground next to the well, and on top of the well using a Trimble R8s RTK-GPS (± 0.5 cm horizontal and ± 2.0 cm vertical; VanDusen et al., 2016). The wells were relatively stationary throughout the study period, moving vertically between sensor readouts a maximum of 0.01 ± 0.04 m at Shackleford Banks, 0.06 ± 0.04 m at Core Banks, and 0.02 ± 0.04 m at Onslow Beach (± 1 SD). A reference water level was determined by measuring the distance from the top of the well to the water surface and survey information was used to convert observed water levels to the North American Vertical Datum of 1988 (NAVD88; VanDusen et al., 2016). Water-level data were processed using HOBOware Pro software and corrected for changes in barometric pressure at Shackleford and Core banks using meteorological NOAA station 8656483, located 14 and 18 km away, respectively, and at Onslow Beach using a barometric pressure sensor deployed at the site (Fig. 1).

2.1.2. *Topographic surveys*

The topography of the Core and Shackleford Banks sites were surveyed on the same day using an Unoccupied Aerial System (UAS). We used a small fixed-wing senseFly eBee Plus equipped with a survey-grade RTK-GPS system and a 20 megapixel Sensor Optimized for Drone Applications (SODA) RGB camera to capture overlapping images of the

sites with < 3 cm ground sampling distance. The images were collected and processed following Seymour et al. (2018). Briefly, the software program Pix4D Mapper was used to generate point clouds from UAS imagery georeferenced using geotags embedded in the image EXIF data, anchored with 4–6 ground control points, and surveyed using the Trimble R8s RTK-GPS. Point clouds were generated through structure from motion (SfM) photogrammetric processing and an inverse-distance weighted method to generate digital surface models (DSM). In total, 14 high-resolution and accuracy (0.03 m ground sampling distance, 0.05 m vertical error) DSMs (7 at Core Banks and 7 at Shackleford Banks) were generated between April 2017–December 2017 (see Supplementary Table).

Beach morphology at Onslow Beach was surveyed January 2012–October 2014 with a Riegl three-dimensional LMSZ210ii terrestrial laser scanner using the same methods outlined in Theuerkauf and Rodriguez (2014). We were unable to deploy a UAS at Onslow Beach because the airspace is restricted and managed by Marine Corps Base Camp Lejeune. The site was scanned in two locations on the foreshore within 2 h of low tide to maximize data coverage. Data points were georeferenced using at least 7 reflector targets surveyed with the Trimble R8s RTK-GPS, with vertical error < 0.03 m. A total of 15 surface grid models (horizontal and vertical error ~0.03 m) were created throughout the time period and imported into Golden Software's Surfer 10.0 to generate elevation models.

For each DSM, x, y, and z data were extracted for every cell along cross-shore transects, projected from the most seaward point of the datasets landward, through the location of the well (Fig. 1). Along the transects we defined the dune crest elevation (D_{High}) as the highest elevation, the dune toe elevation (D_{Low}) where the largest break in slope exists, and slope (slope = β or tan θ; see Fig. 2) using a linear regression fit to data points between the dune toe elevation and mean high water (MHW; Fig. 2; Stockdon et al., 2007; Burroughs and Tebbens, 2008; Doran et al., 2015). Based on NOAA gauges 8656483 and 8658163, MHW is 0.36 m NAVD88 for Core and Shackleford Banks and 0.43 m NAVD88 for Onslow Beach, respectively (Fig. 1). At the Core Banks Site, β includes a gently landward sloping backshore, only inundated during storms and spring tides. Some topographic surveys at Core Banks (April, May, June, July, and September) and Shackleford Banks (April and October) did not extend to the MHW line because data were collected during a period when the water level exceeded MHW (camera cannot image below the water surface). For those surveys, β was calculated to the lowest possible elevation, ~0.10–0.80 m higher than MHW. To evaluate if our measured beach morphology at each site was unique to those observation periods, we extracted the same topographic profiles from available annual historic surveys provided by NOAA Digital Coast (1996–2016).

2.2. Model inputs

2.2.1. Calculating high runup elevation (R_{High}) and characterizing beach state

The total water elevation on the beach is approximated as the high runup elevation (R_{High}). Calculating R_{High} requires estimating $R_{2\%}$ (the 2% exceedance wave-runup elevation) and water level (tide + storm surge; Fig. 2; Holman, 1986; Sallenger, 2000). We used an empirical relationship to estimate $R_{2\%}$, which depends on deep water wave height (H_0), wavelength (L_0), and β (Holman, 1986; Sallenger, 2000; Stockdon et al., 2006) where:

$$R_{2\%} = 1.1\left(0.35\beta\,(H_0L_0)^{1/2} + \frac{[H_0L_0(0.563\beta^2 + 0.004)]^{1/2}}{2}\right)$$

The equation includes setup and swash, and L_0 is calculated as $gT_0^2/2\pi$, where T_0 is wave period (Holman, 1986; Sallenger, 2000; Ruggiero et al., 2001; Stockdon et al., 2006). Beach state, characterized as being more dissipative or reflective, can be determined by both β and wave characteristics over time. Beach state is commonly quantified by the non-dimensional Iribarren Number (ξ_0), parameterized as $\beta/(H_0/L_0)^{1/2}$ with increasing ξ_0 indicating more reflective beaches and we relied on that metric to determine beach state in this study. (Battjes, 1974; Wright and Short, 1983; Short, 1999; Ruggiero et al., 2001; Senechal et al., 2011).

Water level (tide + storm surge) and wave information (T_0 and H_0) were extracted from ADCIRC + SWAN model hindcasts for the collision and overwash time periods identified in the photos (EST, NAVD88). ADCIRC solves for water levels and currents at a range of scales, using the vertically integrated shallow-water equations on an unstructured triangular mesh (Luettich and Westerink, 2004; Atkinson et al., 2004; Dawson et al., 2006; Westerink et al., 2008; Dietrich et al., 2011). The SWAN model utilizes the action balance equation where the rate of change and propagation of wave action are balanced by wind generation and dissipation from bottom friction and white capping (Booij et al., 1999; Stockdon et al., 2007; Dietrich et al., 2011). A node was selected from the ADCIRC + SWAN grid near each study site (Fig. 1) at approximately the 20-meter bathymetric contour to minimize impacts from wave shoaling following Holman (1986).

2.2.2. Defining the impact regimes

The storm impact scale (Sallenger, 2000) was used to examine the relationship between changing beach morphology and R_{High} (Fig. 2; Holman, 1986; Sallenger, 2000). This study specifically focused on

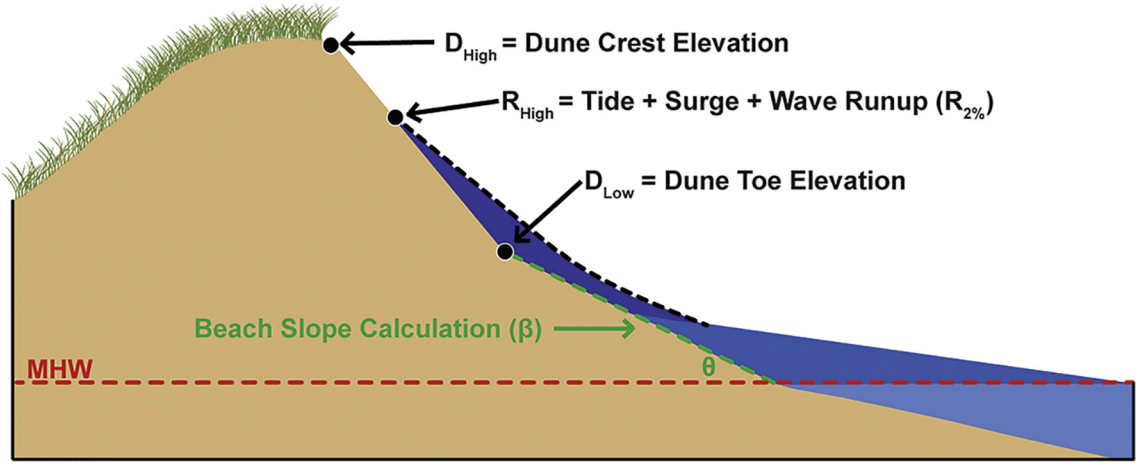

Fig. 2. An illustration of the collision regime showing D_{High}, R_{High}, D_{Low}, MHW, and β. (Modified from Sallenger, 2000 and Stockdon et al., 2007).

predicting the collision and overwash regimes using the Stockdon et al. (2007) model. Collision was only observed at Core and Shackleford Banks and is defined as $D_{Low} < R_{High} < D_{High}$, where D_{Low} and D_{High} are the dune toe and dune crest elevations, respectively. At Onslow Beach, we observed the overwash storm impact regime, defined as $R_{High} > D_{High}$ (Fig. 2; Sallenger, 2000; Wang and Briggs, 2015).

2.2.3. Comparing predicted and observed impact regimes

Using the most recent measurements of β, we calculated R_{High} every hour, compared R_{High} with D_{Low} and D_{High} to determine the predicted impact regime, and compared that predicted impact regime with the photographic record. We evaluated the accuracy of predicting the impact regime at the daily time scale; therefore, if R_{High} reached or exceeded the D_{Low} elevation at any time during a given day, predicted collision or overwash was recorded, and compared with camera photos and water level data. The impact regime was underpredicted when collision was recorded in the photos, but R_{High} was $< D_{Low}$ (swash regime), and when overwash was recorded in the photos and $D_{Low} < R_{High} < D_{High}$ (collision regime). The impact regime was overpredicted when swash was recorded in the photos but R_{High} was $> D_{Low}$ or D_{High} (collision or overwash regimes), and when collision was recorded in the photos but R_{High} was $> D_{High}$ (overwash regime).

2.3. Error assessment

Measurement error associated with D_{Low}, D_{High}, and β values are small because vertical error associated with ground-controlled digital elevation models is only 0.05 m (Seymour et al., 2018). The larger uncertainty associated with the topography data is likely related to unmeasured changes in beach and dune morphology that occurred between when a survey was conducted, and when a collision or overwash event occurred. The accuracy of the water-level information (tide + storm surge) that the ADCIRC model provides, likely varies under different weather conditions, such as a hurricane directly impacting the coast versus high water during a fair-weather spring tide. To evaluate differences in observed and modeled water-level elevation during the identified collision event time periods in 2017 and 2018, water levels from the Wrightsville Beach NOAA gauge 8658163 were compared to ADCIRC water levels extracted from a node near the gauge (Figs. 1 and 3A), which resulted in a root mean squared error (RMSE) of 0.16 m.

Stockdon et al. (2006) calculated a RMSE of 0.32 m for the expression of $R_{2\%}$ assuming known forcing conditions. For our study, the largest uncertainty associated with calculating $R_{2\%}$ is associated with modeling H_0 and T_0, possibly due to the propagation of long period swell generated outside of the ADCIRC + SWAN domain. To calculate differences in observed and modeled offshore wave data during the identified collision event time periods in 2017 and 2018, H_0 and T_0 from the NOAA National Data Buoy Center station 41159 were compared to SWAN output extracted from an ADCIRC + SWAN node ~9 km from the buoy (Figs. 1, 3A, and B). This error analysis has fewer data points than the water-level error analysis because the buoy was inoperable during September and October 2017 (data for those months are missing). The observed versus modeled H_0 and T_0 show an error of 21.6% and 24.2%, respectively. Adding all the uncertainties associated with calculating R_{High} in quadrature, including $R_{2\%}$, tide, and storm surge, results in an error that ranges between 0.37 and 1.08 m for the various waves and beach slopes captured during the events in this study.

Camera trap photos were also used to assess uncertainty associated with calculating R_{High}. Photos collected during shifts in the storm impact regime captured the time when total water elevation first impacted D_{Low} or exceeded D_{High} (within 5 min at Core and Shackleford banks and 2 min at Onslow Beach). Assuming little change in dune morphology since the most recent beach survey, at the time a camera captures the initial storm impact regime shift from swash to collision

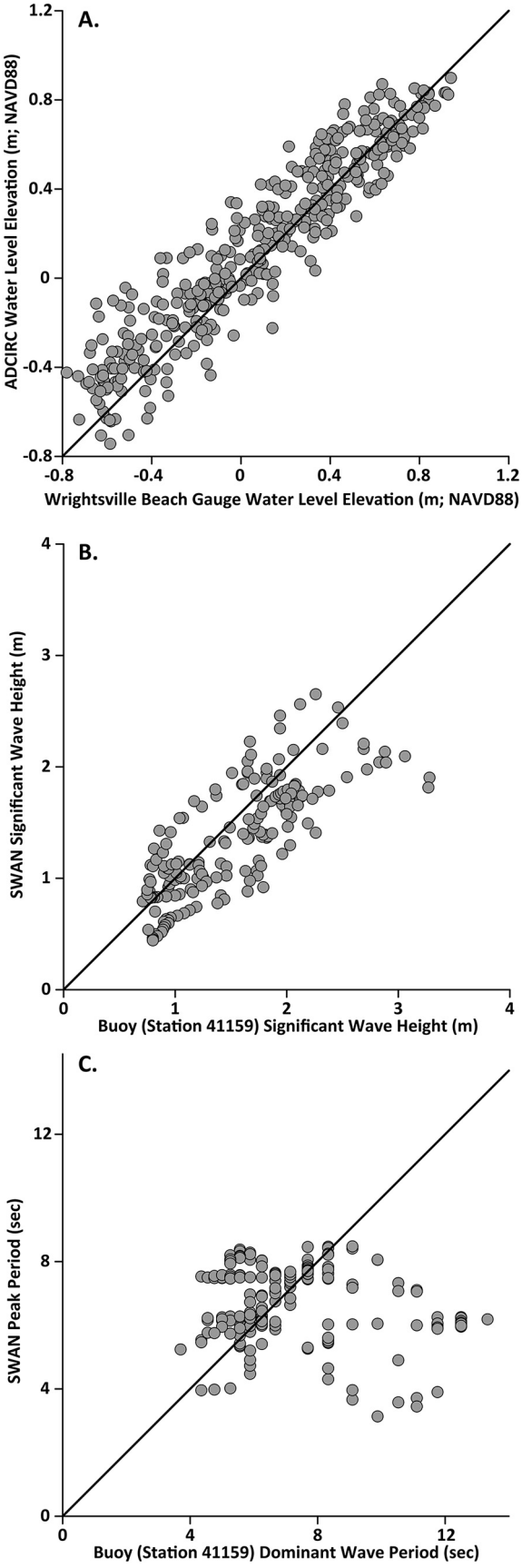

Fig. 3. Hindcast ADCIRC water-level predictions compared to water-level observations at the Wrightsville Beach NOAA gauge station 8658163 (A). Hindcast SWAN significant wave height (B) and peak period (C) predictions compared to observations of significant wave height and dominant wave period at the offshore NOAA buoy station 41159. See Fig. 1 for station location.

and from collision to overwash, the total water elevation should equal D_{Low} and D_{High}, respectively. We derive an assessment of model skill at the initial time of impact regime transition as D_{Low} - R_{High} and D_{High} - R_{High}, which we label as the Regime Transition offset (RTo). Since the photos document the impact regime, negative and positive RTo values represent overprediction and underprediction, respectively. The regime transition was not always captured in our observations at the sites because it sometimes corresponded with periods of darkness when the camera was not operating.

2.4. Accuracy of predicting collision impact regime

It is particularly important to evaluate the accuracy of the Stockdon et al. (2007) model for predicting the collision regime. Dune erosion is commonly associated with storm impact regimes that exceed swash, and collision occurs frequently, being on the lower end of the storm impact scale and a precursor to overwash and inundation. The accuracy of predicting collision by comparing R_{High} and D_{Low} was assessed using a presence/absence model of sensitivity and predictive power reported as a percent (Fielding and Bell, 1997; Congalton and Green, 1999; Stockdon et al., 2007). Sensitivity is the probability that collision will occur and is calculated as the ratio between the number of days collision was predicted correctly (when observational data and predicted data showed collision on the same day) versus the total number of days collision was observed (Stockdon et al., 2007). The predictive power measures the predictive capabilities of the Stockdon et al. (2007) model (used to compute R_{High}) and is calculated as the ratio between the number of days collision was predicted correctly versus the total number of days collision was predicted (Stockdon et al., 2007).

3. Results

3.1. Beach morphology changes

During the study periods that extended from August 2017 to March 2018 for Core and Shackleford Banks and June 2012 to December 2014 for Onslow Beach, β and D_{High} varied by different extents among the sites (Fig. 4). The average D_{High} was greatest at the Core Banks Site (D_{High} = 4.61 ± 0.09 m; D_{Low} = 2.15 ± 0.18 m; ± 1 SD), intermediate at the Shackleford Banks Site (D_{High} = 2.96 ± 0.15; D_{Low} = 1.77 ± 0.53; ± 1 SD) and lowest at the Onslow Beach Site (D_{High} = 1.44 ± 0.27; D_{Low} = 0.99 ± 0.28; ± 1 SD; Fig. 4). The average β was highest at the Shackleford Banks Site, intermediate at the Onslow Beach Site and lowest at the Core Banks Site (Fig. 5). The lower dune elevations and beach slopes at the Onslow Beach Site is the result of a large washover fan that formed following Hurricane Irene in August 2011 (VanDusen et al., 2016; Theuerkauf and Rodriguez, 2017). At all sites β, D_{Low}, and D_{High} do not change in a consistent direction through time, rather, measurements increase and decrease over the study periods (Fig. 4). Additionally, the Core Banks Site showed the least variability in D_{High}, D_{Low}, and β as compared to the sites at Shackleford Banks and Onslow Beach (Fig. 5).

In comparison to the previous two decades, the elevations of D_{High} during the study periods were on average 1.2 m (28.5%) higher at Core Banks, 0.5 m (17.6%) higher at Shackleford Banks, and 0.8 m (42.6%) lower at Onslow Beach (Fig. 5 and Table 1). The large percent difference in D_{High} at Onslow Beach was the result of storms eroding the relatively narrow dune line prior to our study period. At the Core and Shackleford Banks sites, average β calculated in 2017 was ~0.02 lower and within the error of the average β (± 1 SD) calculated from the historical data over the past 17 years (0.04 ± 0.01), and 18 years (0.10 ± 0.04), respectively. At the Onslow Beach Site, average β calculated using our data from 2012 to 2014 was ~0.02 higher than the calculated average β from 20 years of historical data (0.04 ± 0.02). The historical beach slopes and D_{High} elevations measured at Core and Shackleford Banks showed larger variances than our dataset (Fig. 5),

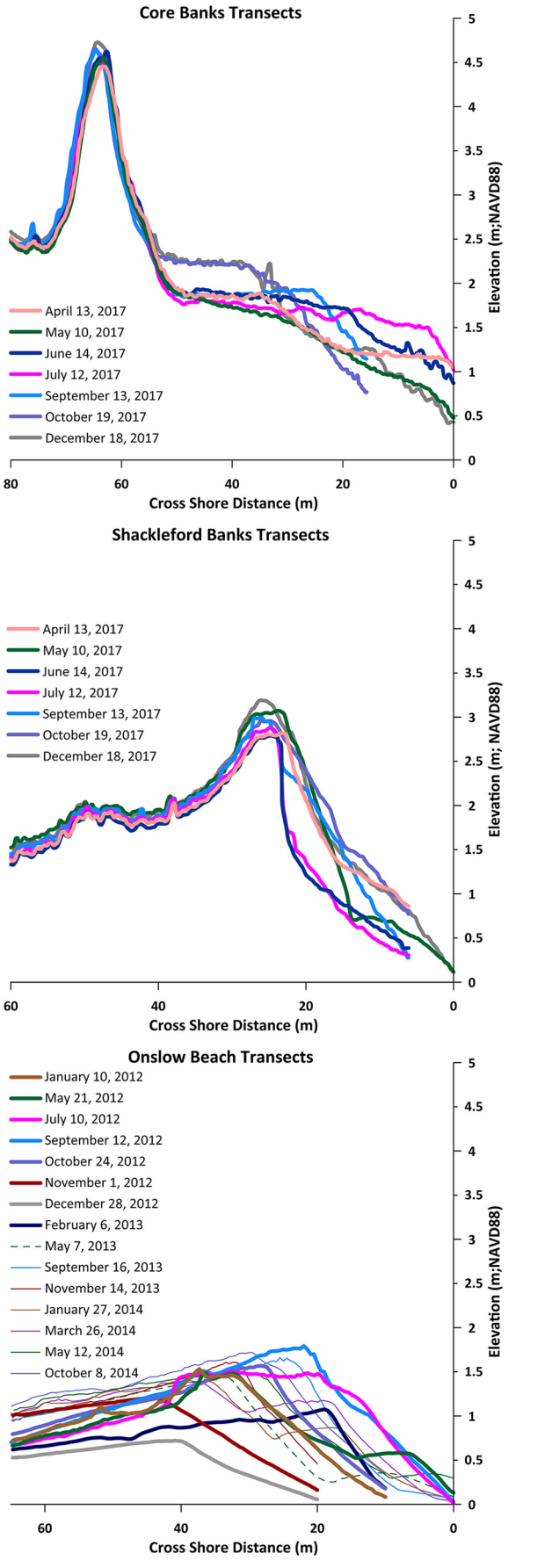

(caption on next page)

Fig. 4. Cross shore beach transects for all topographic surveys obtained for this study at each site showing changes in beach morphology through time. Cross shore distance is measured from a common zero point on the foreshore. Notice different horizontal scales. See Fig. 1 for locations.

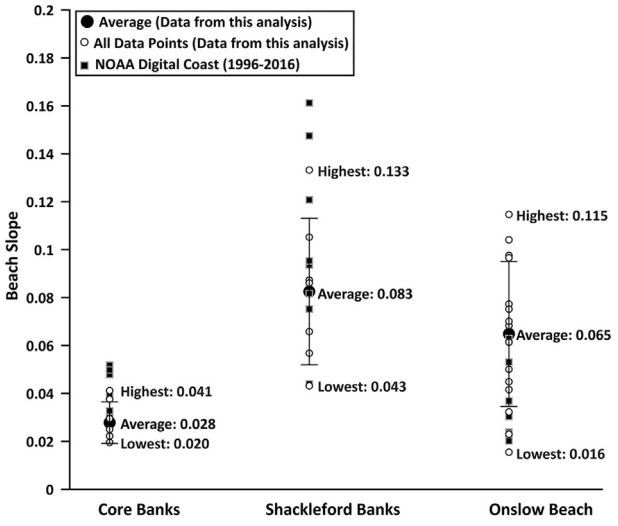

Fig. 5. Average beach slope (β) ± 1 SD (black circles) of all slope data measured in this study (white circles). Slope data obtained from NOAA digital coast for available years from 1996 to 2016 (black squares) are also shown.

likely because the historical data was commonly obtained following major storm events, such as Hurricanes Floyd (1999), Irene (2011), Sandy (2012), and Matthew (2016), and using lower resolution airborne LiDAR data (± 0.20 m vertical). The opposite was the case at Onslow Beach since Hurricane Irene impacted the area in August 2011 and caused frequent overwash and topographic change during our study period (VanDusen et al., 2016).

Using data obtained during our event time periods, (Table 2) average ξ_0 for Core Banks, Shackleford Banks and Onslow Beach were 0.36 ± 0.17, 1.08 ± 0.41, and 1.48 ± 1.57 (± 1SD), respectively. Those ξ_0 numbers are variable but generally show Core Banks as the most dissipative beach, and Onslow Beach and Shackleford Banks being intermediate (more reflective; Fig. 6). Onslow Beach had a lower average slope as compared to Shackleford Banks, but its higher average Iribarren number is a result of long waves during the Hurricane Sandy event (October 24–29, 2012; Fig. 6). Excluding Hurricane Sandy, Onslow Beach and Shackleford Banks have similar average Iribarren numbers. The historical dataset of site morphology shows similar beach-slope trends as our measurements, where the Core Banks Site had the lowest and least variable beach slopes as compared to the Shackleford Banks and Onslow Beach sites, indicating beach states of more dissipative and intermediate beaches have been consistent over at least the past two decades.

3.2. Predicted and observed impact regime

We captured 10 collision and overwash events in total, the events ranged from 1 to 6 days in duration, and topography data were collected an average of 38 days before an event occurred with a range between 1 and 100 days (Table 2; Figs. 7–9). All of the events observed at Core and Shackleford Banks were included in the study (Events 3–10); however, we had to limit events at Onslow Beach to include only Hurricanes Isaac (August 26–31; Event 1) and Sandy (October 24–29; Event 2) because at the time Onslow Beach was surveyed ADCIRC + SWAN data were only being archived for Hurricanes. The Onslow Beach Site experienced overwash during Event 1 even though Hurricane Isaac had minimal impact on the North Carolina coast (Fig. 8). The storm mainly impacted the Gulf of Mexico, but since the Onslow Beach Site was within the ADCIRC + SWAN model domain, we had access to wave and water-level outputs. Events 4 and 5 produced collision events at both Core and Shackleford Banks. These events during September 15–19, and September 23–27 were from Hurricane Irma (Event 4) and Hurricanes Jose and Maria (Event 5; Fig. 7), respectively. In addition to those hurricanes, six short-duration (1–3 day) periods of collision (events 3 and 6–10) occurred at the Shackleford Banks Site that were the result of onshore-directed wind and high tide (Table 2). The impact regime was occasionally underpredicted by R_{High} during three days at Shackleford Banks (Events 6, 8, and 10) and one day at Onslow Beach, excluding positive error (Event 1; Fig. 9). Overprediction of the impact regime by R_{High} was more common and occurred for three days on Core Banks, 10 days on Shackleford Banks, and 3 days on Onslow Beach (Events 1, 2, 4, and 5, Fig. 9). During photo-documented collision and overwash events, the loggers did not always record a water level > D_{Low} because they could not capture the maximum elevation of wave runup (Figs. 7 and 8) due to their low sampling rate (5 min) and placement at a lower elevation than D_{Low} on the backshore (Core Banks), foreshore (Shackleford Banks), or behind the dunes (Onslow Beach).

The R_{high} was different at Core and Shackleford Banks during events 3–5 (Figs. 7 and 9), largely due to differences in shoreline orientation (different water levels were predicted by ADCIRC; Fig. 1). Event 3 only occurred at the Shackleford Banks Site because strong southerly winds (6.7–10.3 m sec^{-1}) raised the water level above D_{Low} and shifted the impact regime from swash to collision, which was captured in R_{High}, camera photos, and water-level logger data (Fig. 7C). Notably, during Event 3 collision neither occurred nor was predicted at the east-facing Core Banks Site. Both Core and Shackleford Banks were predicted to be in the collision and overwash regimes, respectively, during Event 4 (Hurricane Irma) and Event 5 (Hurricanes Jose and Maria); however, the sites only experienced collision that was close to the threshold between swash and collision (Figs. 7A, B, and 9). Differences in the impact regime experienced by Core Banks (collision) and Shackleford Banks (swash) during the end of Event 5 on September 26, were due to the strong (12.3–18.0 m sec^{-1}) north-northeasterly wind direction that increased surge more at the Core Banks Site than the Shackleford Banks Site. Those differences, however, were not captured in R_{High} that correctly predicted the collision regime for Core Banks, but overpredicted an overwash regime for Shackleford Banks (Figs. 7A, B, and 9). At Shackleford Banks, on average D_{High} is 35% lower and β is 196% higher than Core Banks. These morphologic differences make the threshold for the occurrence of collision and overwash lower at Shackleford Banks than at Core Banks. Consistent with these differences, Shackleford Banks experienced more collision events than Core Banks over the same time period.

Overwash and swash were the only impact regimes identified on the

Table 1
Comparison of the minimum, average, and maximum D_{High} and D_{Low} from the NOAA Digital Coast historical data (1996–2016) and the data obtained for this study.

Study site	D_{High} elevation (m) from historical data. min., avg., max.	D_{Low} elevation (m) from 8 avg., max.	D_{High} difference (historical - this study) min., avg., max.	D_{Low} difference (historical - this study) min., avg., max.
Core	2.7, 3.5, 4.5	1.6, 2.1, 2.4	0.3, 1.2, 1.8	0.0, 0.1, 0.4
Shackleford	1.7, 2.5, 2.9	0.7, 1.3, 1.9	0.3, 0.5, 1.1	0.1, 0.4, 0.6
Onslow	1.4, 2.2, 3.0	0.5, 1.2, 1.6	0.7, 0.8, 1.2	0.1, 0.2, 0.3

Table 2
Events observed at each site during this study.

Event #	Study site	Period	Days (#) since beach surveyed	Principle driver	Maximum observed impact regime
1	Onslow	August 26–31 2012	47	Hurricane Isaac	Overwash
2	Onslow	October 24–29 2012	1	Hurricane Sandy	Overwash
3	Shackleford	August 29 2017	46	Wind	Collision
4	Shackleford & Core	September 15–19 2017	3	Hurricane Irma	Collision
5	Shackleford & Core	September 23–27 2017	10	Hurricanes Jose and Maria	Collision
6	Shackleford	October 24 2017	5	Wind	Collision
7	Shackleford	November 19 2017	31	Wind	Collision
8	Shackleford	December 12 2017	62	Wind	Collision
9	Shackleford	March 7 2018	79	Wind	Collision
10	Shackleford	March 28–30 2018	100	Wind	Collision

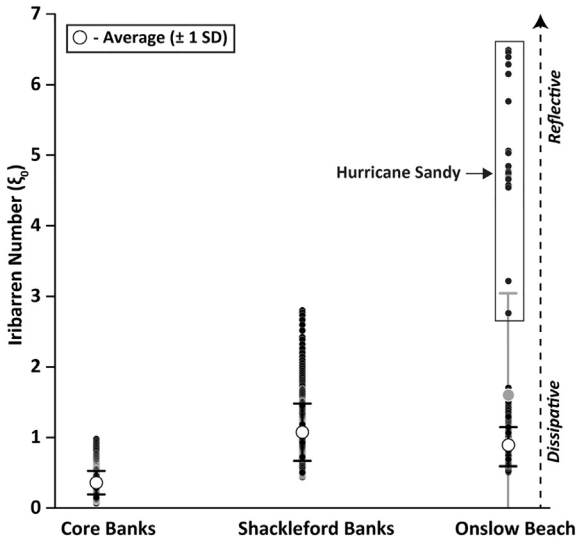

Fig. 6. The Iribarren number (ξ_0) was calculated at each site using the most recent beach morphology data and H_0 and L_0 values obtained from the SWAN model for the 10 events captured during the study periods (see Fig. 1). Despite the high variability of ξ_0 at and among the sites, on average, Core Banks is the most dissipative beach with Shackleford Banks and Onslow Beach being intermediate (more reflective). The average ξ_0 for Onslow Beach was calculated with and without data from Hurricane Sandy noted in gray and black, respectively.

photos and logger data at Onslow Beach (Figs. 8 and 9). This is consistent with the low threshold for overwash at Onslow Beach because of the low average elevation of D_{High} and D_{Low} at 1.44 and 0.99 m NAVD88, respectively (mean high water is ~0.43 m NAVD88) and relatively high β (Fig. 5). During events 1 and 2, overwash was observed and predicted by R_{High} for four days during each event, as Hurricanes Isaac (Event 1) and Sandy (Event 2) passed landward and seaward of the site, respectively (Fig. 9). Dune erosion during Event 1, decreased the elevations of D_{High} and D_{Low} making the site even more vulnerable to overwash during Event 2 (Fig. 4).

3.2.1. Regime transition offset

The average absolute value of RTo during events 1 and 2 at Onslow Beach was 0.27 m and 1.31 m, respectively (Table 3). Event 1 was caused by an onshore-directed wind event (average wind speed 4.2 m sec^{-1} and H_0 1.3 m) from Hurricane Isaac passing far inland of the site, while the larger |RTo| during Event 2 (all values are negative indicating overprediction) coincides with Hurricane Sandy passing offshore of the site with a H_0 of 4.65 m in Onslow Bay and offshore directed winds of 10.8 m sec^{-1} (information from NOAA Buoy 41159). At Shackleford Banks during hurricane-induced events 4 and 5, RTo ranged from −1.29 to −2.13 m (overprediction), but the events at Shackleford Banks that were not caused by large storms such as event 3, 6, 8, 9, and 10 had much lower average values of RTo ranging from 0.26 m to 0.91 m (underprediction). Event 5 at Core Banks had an average RTo of only −0.44 m, less negative than Shackleford Banks. Values of |RTo| and the error associated with R_{High} increased during hurricanes at Onslow Beach and Shackleford Banks and the sign of the RTo values during hurricanes generally indicate overprediction (negative; Fig. 9; Table 3).

3.2.2. Collision prediction accuracy

On some days when collision was observed, R_{High} increased above D_{Low} and subsequently above D_{High}, leading to prediction of an overwash regime. To account for this, we calculated sensitivity and predictive power using two different approaches. The first approach includes days when collision was observed, and only predicted ($D_{Low} < R_{High} < D_{High}$). The second approach includes days when collision and/or overwash impact regimes were observed and predicted ($R_{High} > D_{Low}$). Negative uncertainty was ignored in all assessments to avoid overstating the predictive power and sensitivity of the model. To examine the impact of changing beach morphology on model sensitivity and predictive power, R_{High} was calculated during the events with the most recent, lowest, average, and highest pre-storm β measured, which resulted in a range of percentages for most of the scenarios (Table 4).

At Core Banks, the sensitivity of the Stockdon et al. (2007) model was consistently 100%, regardless of which β we used as input, indicating that the model correctly predicted collision every day it was observed (Table 4). The predictive power of the Stockdon et al. (2007) model at Core Banks was consistently 67%, despite changing β, because three of the nine days collision was predicted by R_{High}, the site was in the swash impact regime (Table 4 and Fig. 9). During those three days when the model overpredicted collision, R_{High} was only between 0.39 and 0.26 m above D_{Low}, within the 0.51–0.55 m uncertainty, therefore, if we had accounted for model uncertainty in the negative elevation direction, then the predictive power would have been 100%.

At the Onslow Beach Site, model sensitivity and predictive power for the collision impact regime could not be calculated because collision was too brief to be observed in the photos at that site. When the overwash impact regime was included in the analysis, sensitivity and predictive power at the Onslow Beach Site was 89–100% and 67–75%, respectively, and invariant using the range of β values observed during the study period as model input (Table 4). The predictive power at Onslow Beach was < 100% because R_{High} overpredicted the impact regime for three days and underpredicted the impact regime for one day (Fig. 9). These mismatches were within 0.10 m and 0.13 m of the overwash impact regime thresholds (D_{High}) when the most recent β was used and within the 0.37–0.39 m uncertainty of the model.

At Shackleford Banks, model sensitivity and predictive power were generally lower than the other sites and degraded as R_{High} was calculated with different values of β (Table 4). The model overpredicted the observed swash and collision impact regimes when using the most recent slope for events 4 and 5. Overpredictions of those events were 0.11 m to 2.58 m above D_{Low} and 0.54–1.08 m above model

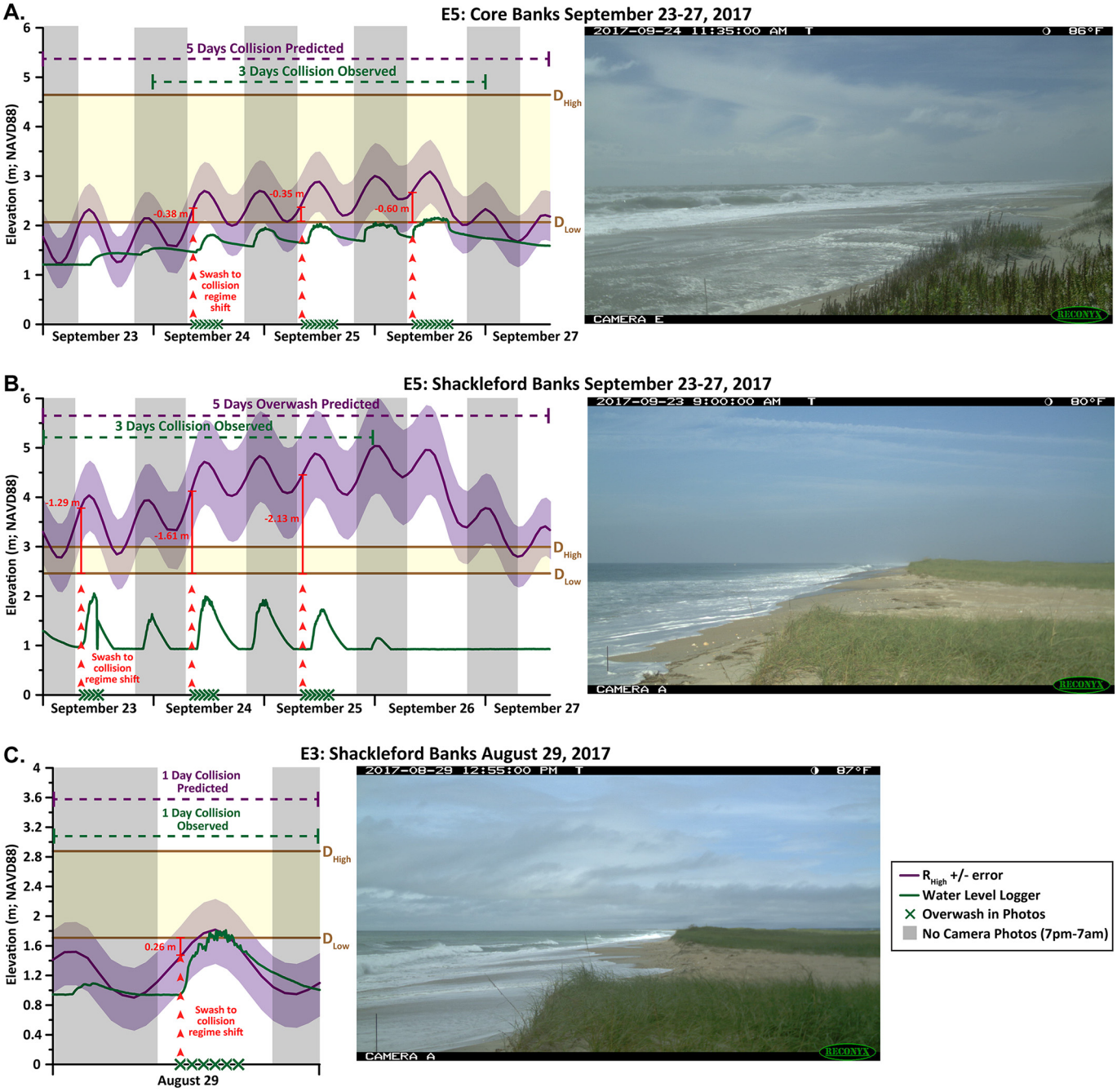

Fig. 7. Examples of recognizing storm impact regimes from observations and predictions. Collision was observed at both Core (A) and Shackleford Banks (B) during Event 5, but only at Shackleford Banks during Event 3 (C). Regime Transition offset (RTo) values were calculated at the time collision was first observed at the sites using D_{Low} - R_{High} (shown in red). The photos are showing collision at Core and Shackleford Banks. (For interpretation of the references to color in this figure legend, the reader is referred to the web version of this article.)

uncertainty, except for on September 15 and 27. The model underpredicted the collision impact regime during events 6, 8, and 10 from 0.16 m to 0.30 m below D_{Low} when the most recent β was used, but those underpredictions were within the 0.42 to 0.47 m model uncertainty. When predictions of collision and overwash were included in the analysis of the Shackleford Banks Site, sensitivity generally increased but predictive power decreased because overwash was never observed at the site, but was predicted for many days (Table 4, Fig. 9). Using the highest β value at the Shackleford Banks Site, the sensitivity and predictive power for collision and overwash was 100% and 67%, respectively, because the highest β elevates R_{High} for events 6, 8, and 10 into the collision regime.

4. Discussion

4.1. Crossing impact regime thresholds

Predicting when storm impacts above the swash regime will occur along beaches and likely cause dune erosion, is important for coastal communities that rely on dunes for protection from coastal flooding. The utility of the Stockdon et al. (2007) model for predicting impact regimes above swash increases with predictive power and with an understanding of the model's limitations, which are mainly related to the quality of the inputs. Using the most contemporaneous β obtained prior to an event, the Stockdon et al. (2007) model overpredicted and

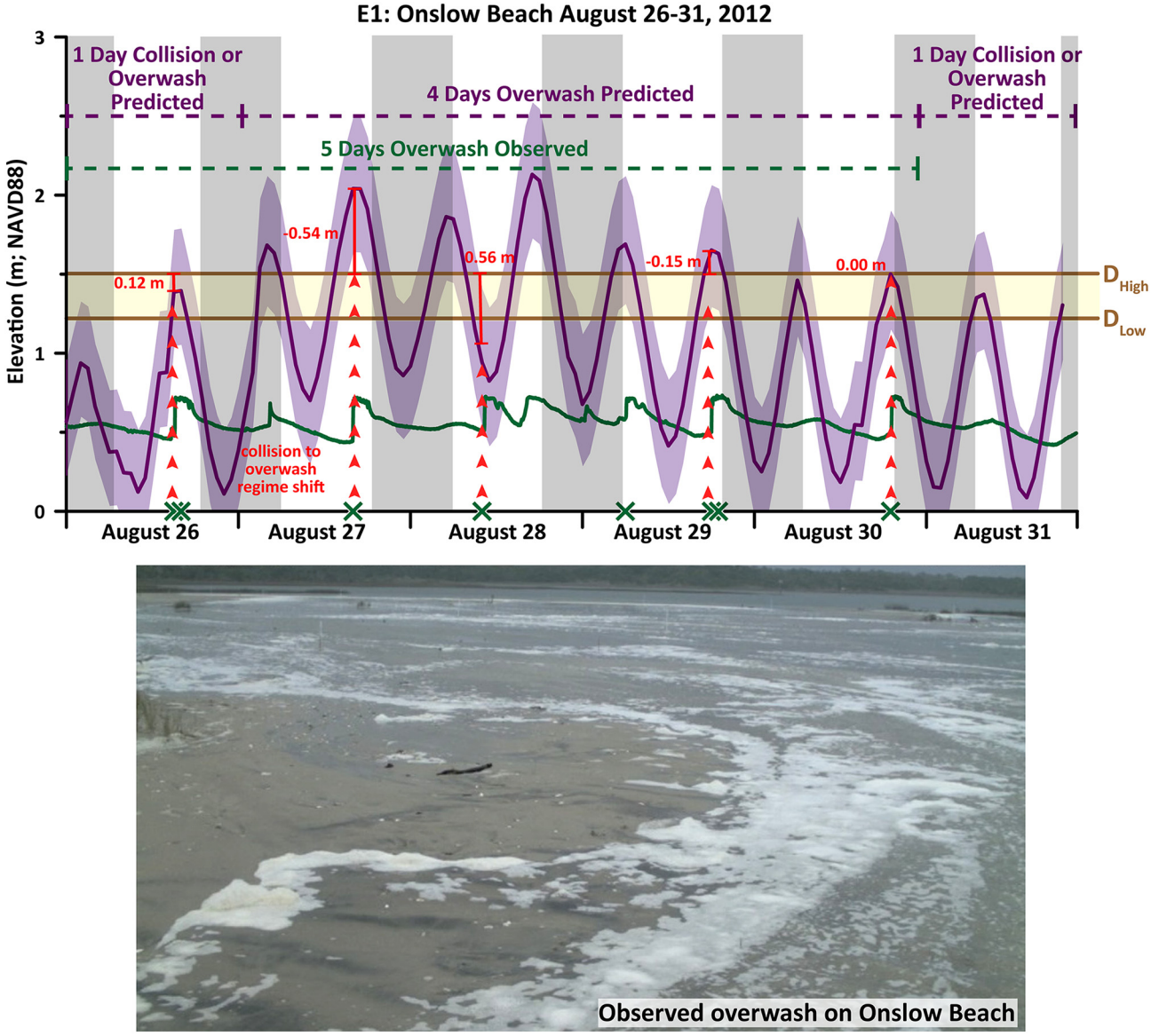

Fig. 8. Example of recognizing the storm impact regime at Onslow Beach from observations and predictions. Regime Transition offset (RTo) values were calculated at the time overwash was first observed at the sites using D_{High} - R_{high} (shown in red) The photo was taken looking landward and shows the intracoastal waterway in the background. See Fig. 7 for legend. (For interpretation of the references to color in this figure legend, the reader is referred to the web version of this article.)

underpredicted the impact regime by < 0.40 m, which was within the 0.37–1.08 m error estimate for R_{High}, except during hurricane-induced events 4 and 5 at Shackleford Banks when overprediction was much higher (Fig. 9). The accuracy of R_{High} was generally lower for hurricanes associated with large surge and waves moving up the coast (events 2, 4, and 5) than the more common localized strong onshore winds with smaller surge and wave conditions. The accuracy of R_{High}, however, could not be measured directly because our water-level loggers were unable to record maximum runup elevations. The photo-based RTo provides an additional benchmark for the accuracy of R_{High} and the average absolute value of RTo for all observations was 0.78 m, which is close to and helps validate the midpoint value of the R_{High} error estimate (0.73 m, Table 3 see methods). The |RTo| and the error associated with R_{High} both increased during Hurricanes at Onslow Beach and Shackleford Banks (Fig. 9 and Table 3), indicating that the Stockdon et al. (2007) model is less accurate during large storms then it is during smaller events at more reflective beaches, and this is likely caused by changes in β that occur during large events that are not constrained.

Large wave events tend to lower β, especially in the case of more reflective sandy beaches while dissipative beaches are more resistant to changes in β over short time periods (hours; Wright, 1980; Wright and Short, 1983; Newe et al., 1999; Aagaard et al., 2005). At the more reflective Shackleford and Onslow Beach sites, a likely decrease in β during Events 2, 4, and 5 was neither captured in our field data nor input into the model and may have resulted in overprediction of the impact regime. The calculation of $R_{2\%}$ is sensitive to β because wave-energy dissipation reduces runup. If $R_{2\%}$ is based on a high β measured before an event occurs and that β is subsequently reduced during a storm associated with large waves, but not captured in the dataset, then the calculation of R_{High} is more likely to overpredict the total water elevation. This is the situation at Shackelford Banks where the impact regime was consistently overpredicted during events 4 and 5 (caused by hurricanes passing by the site) and $R_{2\%}$ was calculated using the highest β observed during the study period (0.133, Fig. 9). Changes in wave direction and water levels around the Cape Lookout Bight, which are not captured at the offshore node where we sampled the ADCIRC + SWAN model output, also likely contributed to mismatches between the

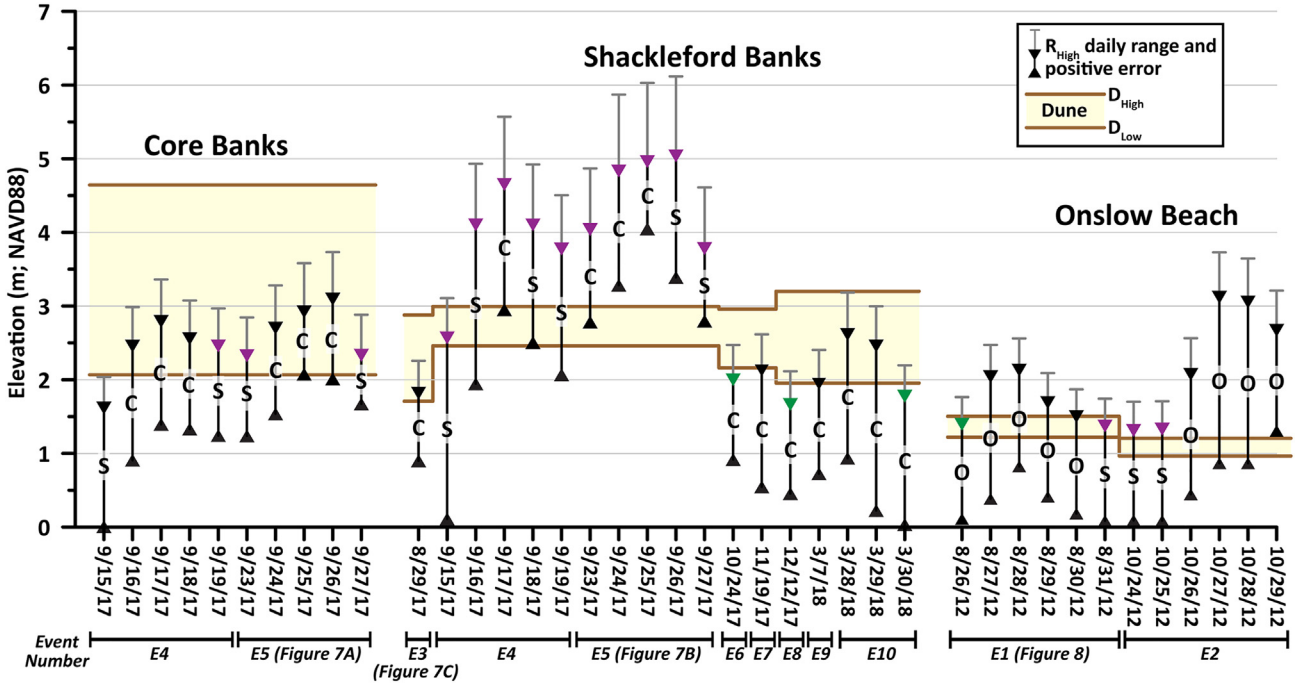

Fig. 9. The 10 events when collision or overwash was predicted or observed are grouped by site from north to south. The daily range of R_{High} during the events (delineated as black vertical bars with positive error associated with R_{High} max. in gray) is compared to changing D_{High} and D_{Low} elevations at the sites (delineated as horizontal yellow bars depicting dune relief). The letters on the R_{High} daily range bars indicate the largest impact regime observed in the photos for that day (S = Swash, C = Collision, O = Overwash). The color of the top arrow on the R_{High} daily range bars indicate that total water elevation was overpredicted (purple), underpredicted (green), and correctly predicted (black). (For interpretation of the references to color in this figure legend, the reader is referred to the web version of this article.)

Table 3
Event days where the Regime Transition offset (RTo) was captured at the sites. The calculation of RTo can be found in Methods.

Event #	Event location	Event day	Regime shift to overwash (m)[a]
1	Onslow Beach	August 26 2012	0.12
1	Onslow Beach	August 27 2012	−0.54
1	Onslow Beach	August 28 2012	0.56
1	Onslow Beach	August 29 2012	−0.15
1	Onslow Beach	August 30 2012	0.00
2	Onslow Beach	October 26 2012	−0.87
2	Onslow Beach	October 27 2012	−1.60
2	Onslow Beach	October 29 2012	−1.46

Event #	Event location	Event day	Regime shift to collision (m)[a]
3	Shackleford Banks	August 29 2017	0.26
4	Shackleford Banks	September 17 2017	−1.78
5	Shackleford Banks	September 23 2017	−1.29
5	Shackleford Banks	September 24 2017	−1.61
5	Shackleford Banks	September 25 2017	−2.13
5	Core Banks	September 24 2017	−0.38
5	Core Banks	September 25 2017	−0.35
5	Core Banks	September 26 2017	−0.60
6	Shackleford Banks	October 24 2017	0.46
8	Shackleford Banks	December 12 2017	0.46
9	Shackleford Banks	March 7 2018	0.35
10	Shackleford Banks	March 28 2018	−0.41
10	Shackleford Banks	March 29 2018	0.91
10	Shackleford Banks	March 30 2018	0.86

[a] Negative value indicates overprediction, positive value indicates underprediction.

observed and predicted impact regimes.

The time between when a beach survey was conducted, and a hurricane caused collision or overwash at our sites ranged between 1 and 47 days. This lag is much shorter than what was used in previous studies (months to years) that also argue outdated pre-storm topography was a large contributor to uncertainty in the model (Stockdon et al., 2007; Long et al., 2014). Incorporating changes in β that occur during events associated with large waves, like hurricanes, will improve impact-regime predictions based on the Stockdon et al. (2007) model. Our surveys of beach morphology were conducted more frequently and closer to when storms conditions were manifested at the sites than what most coastal management programs are designed to achieve (Smith and Benson, 2001), highlighting the need for near real-time information on β for intermediate beach states. During the hurricanes captured in this

Table 4
Model sensitivity and predictive power (accounting for model uncertainty in the positive direction) using different beach slopes from the study periods as shown in Fig. 4. C = collision regime and O = overwash regime.

Study site	C sensitivity	C predictive power	C + O sensitivity	C + O predictive power
Most recent slope				
Core	100%	67%	100%	67%
Shackleford	42–67%	83–100%	75–83%	50–60%
Onslow	N/A	N/A	89–100%	67–75%
Lowest slope				
Core	100%	67%	100%	67%
Shackleford	42%	50–63%	42–50%	46–63%
Onslow	N/A	N/A	89–100%	67–75%
Average slope				
Core	100%	67%	100%	67%
Shackleford	25–33%	50%	58%	44–54%
Onslow	N/A	N/A	89–100%	67–75%
Highest Slope				
Core	100%	67%	100%	67%
Shackleford	42–50%	50–63%	100%	67%
Onslow	N/A	N/A	89–100%	67–75%

study, however, the Stockdon et al. (2007) model tended to only overpredict R_{High} into the overwash impact regime, making it still a useful indicator that the swash impact regime was exceeded.

4.2. Model predictions across beach states

Stockdon et al. (2007) demonstrated alongshore variability in the storm impact regime for two hurricanes that affected North Carolina using the total water elevation (modeled using Delft3D-FLOW and SWAN) and a pre-storm beach survey. Comparing the predicted impact regime with the inferred impact-regime, based on post-storm surveys, resulted in a prediction accuracy of 68.5–74.8% for the overwash regime but only 23.2–44.0% for the collision regime (Stockdon et al., 2007). While the prediction accuracy for the collision regime was higher in our study (Table 4), we benefited from real-time observations of impact state, while Stockdon et al. (2007) had difficulty identifying evidence of collision in the post-storm LiDAR surveys. The Stockdon et al. (2007) model configured here predicted the occurrence of collision better at the Core Banks Site than the Shackleford Banks Site (Fig. 9), despite the predictive power consistently being 67%, because R_{High} at the Core Banks Site never underpredicted the impact regime and the three days of overprediction were always within the range of R_{High} error. Although D_{Low} was similar at Core and Shackleford Banks, the dissipative beach at the Core Banks Site was more resistant to collision due to wave-energy dissipation than the more reflective beach at the Shackleford Banks Site and did not experience an impact regime shift during events 3 and 6–10. The dunes at the Onslow Beach site had the lowest relief (0.24 and 0.28 m) and lowest D_{Low} (0.97 and 1.22 m) making the site highly susceptible to overwash. During Event 2 (Hurricane Sandy), the Stockdon et al. (2007) model did not overpredict the impact regime at the more reflective Onslow Beach Site because of the Site's low resistance to overwash; however, it did overpredict R_{High} by -0.87 to -1.60 m based on the RTo metric (negative RTo = overprediction).

The Stockdon et al. (2007) model tends to overpredict total water elevation during hurricanes at the more reflective Shackleford Banks and Onslow Beach sites than it does during smaller events and at dissipative beaches like Core Banks. In addition to changes in β during storm events, beach slopes at more reflective beaches, such as Shackleford Banks and Onslow Beach, are more dynamic over longer, monthly to yearly timescales than slopes of dissipative beaches. This could be because more reflective beaches experience a wide range of wave heights throughout a year and have a relatively low sediment supply, which results in a high mobility of sediment between the surfzone and subaerial beach (e.g. Short and Hesp, 1982; Masselink and Li, 2001; Ruggiero et al., 2001). Beach sand is consistently < 0.5 m thick at the Onslow Beach Site with the underlying units composed of carbonaceous mud and clay (Rodriguez et al., 2012; Rodriguez et al., 2018). There are other variables that control beach state, however, such as the grain size of beach sediment and depth of underlying stratigraphic units; therefore, not all intermediate-reflective beaches are morphologically dynamic like those along the coastal plain of North America (Jackson et al., 2005).

The $R_{2\%}$ component of R_{High} is sensitive to changes in β, and this sensitivity is exacerbated with increasing H_0 and T_0 (Fig. 10). The Shackleford Banks and Onslow Beach sites show greater variability in β and $R_{2\%}$ than the Core Banks Site (Fig. 10). For example, over the course of this study, the Shackleford Banks and Onslow Beach sites experienced $R_{2\%}$ values of 0.16–5.93 m and 0.12–5.23 m, respectively (Fig. 10). In contrast, the more dissipative Core Banks Site showed less variability in β and experienced $R_{2\%}$ elevations of 0.12–2.78 m, supporting previous work showing wave runup is lessened by wave-energy attenuation due to the low β on dissipative beaches than it is on more reflective beaches (Ruggiero et al., 2001; Figs. 5 and 10). It is likely that the β at Shackleford Banks and Onslow Beach sites decreased during the hurricane-induced events, such as events 2, 4, and 5.

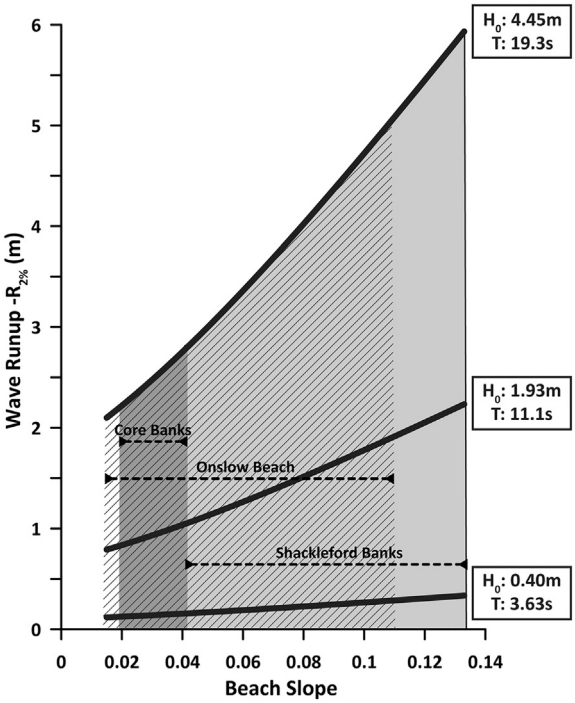

Fig. 10. Wave runup ($R_{2\%}$) versus beach slope comparison. The three bold lines of wave runup versus beach slope represent the lowest, average, and highest wave characteristics experienced during all events as compared to the range of beach slopes measured at Core Banks (dark gray), Shackleford Banks (light gray), and Onslow Beach (diagonal lines), depicted as dashed horizontal lines.

5. Conclusions

Identifying coastal areas that are vulnerable to dune erosion is increasingly important as coastal development expands, and the exposure of coastal communities to ocean flooding increases. Storm impact models that accurately predict impact regimes are an important tool for coastal communities. The applicability of a pre-storm β measurement for accurately configuring a model to predict the storm impact regime is mainly dependent on beach state. Less frequent surveys result in accurate predictions of the storm impact regime at more dissipative beaches like the Core Banks Site, where the model sensitivity and predictive power was invariant with the small morphologic variations captured throughout our study period. More reflective beaches, however, require assessment of beach morphology more often (ideally in real time), especially to capture changes in β that occurred during events. The Stockdon et al. (2007) model tended to overpredict the impact regime during storms with large waves, likely because β decreased during the storm, wave energy was attenuated, and that change was not captured in the configuration of the model.

During all instances when R_{High} underpredicted the impact regime, it was within error, which is likely because H_0 and T_0 were relatively small during those events that were not driven by hurricanes and the beach slopes measured prior to the events and used in calculating R_{High} remained relevant. When R_{High} overpredicted the impact regime at the Core Banks Site, it was always within error; however, overpredictions at the Shackleford Banks Site exceeded error because beach slope likely decreased during the events and waves could have been modified by refraction associated with the Cape Lookout spit. The findings of this work suggest that more accurate information on β collected close in time to an event and devising a means for incorporating β changes that occur in real time during an event into predictions of $R_{2\%}$, may improve predictions of the storm impact regime. Using β values obtained from beach morphology models such as XBeach (Roelvink et al., 2009) or Windsurf (which includes the capability to simulate topographic

recovery; Cohn et al., 2019) between field surveys and for forecasted storm conditions could reduce storm impact regime overpredictions, especially for more reflective beach sites.

Supplementary data to this article can be found online at https://doi.org/10.1016/j.margeo.2020.106201.

Declaration of competing interest

The authors declare that they have no known competing financial interests or personal relationships that could have appeared to influence the work reported in this paper.

Acknowledgements

Beth VanDusen, Carson Miller and Molly Bost assisted in field work. Funding was provided by the National Park Service, the Environmental Security Technology Certification Program (RC18-5187), the Defense Coastal/Estuarine Research Program (DCERP), funded by the Strategic Environmental Research and Development Program (SERDP), and by the UNC Coastal Resilience Center Science & Engineering Workforce Development Grant Program administered by the U.S. Department of Homeland Security Science and Technology Directorate (2015-ST-061-ND0001-01). “The views and conclusions contained in this document are those of the authors and should not be interpreted as necessarily representing the official policies, either expressed or implied, of the U.S. Department of Homeland Security and U.S. Department of Defense.” Presentation of this work was greatly improved from comments and edits provided by three anonymous reviewers.

Data availability

The data are available from the authors by request. The ADCIRC + SWAN data can be obtained from the Coastal Emergency Risks Assessment website (https://cera.coastalrisk.live/).

References

Aagaard, T., Kroon, A., Andersen, S., Møller Sørensen, R., Quartel, S., Vinther, N., 2005. Intertidal beach change during storm conditions; Egmond, the Netherlands. Mar. Geol. 218, 65–80.

Atkinson, J.H., Westerink, J.J., Hervouet, J.M., 2004. Similarities between the wave equation and the quasi-bubble solutions to the shallow water equations. Int. J. Numer. Methods Fluids 45, 689–714.

Battjes, J.A., 1974. Surf Similarity, Paper Presented at 14th Coastal Engineering Conference, Am. Soc. of Civ. Eng., Copenhagen.

Booij, N.R.R.C., Ris, R.C., Holthuijsen, L.H., 1999. A third-generation wave model for coastal regions: 1. Model description and validation. J. Geophys. Res. Oceans 104 (C4), 7649–7666.

Burroughs, S.M., Tebbens, S.F., 2008. Dune retreat and shoreline change on the Outer Banks of North Carolina. J. Coast. Res. 24 (sp2), 104–112.

Casella, E., Rovere, A., Pedroncini, A., Mucerino, L., Casella, M., Cusati, L.A., ... Firpo, M., 2014. Study of wave runup using numerical models and low-altitude aerial photogrammetry: A tool for coastal management. Estuarine, Coastal and Shelf Science 149, 160–167.

Cohn, N., Hoonhout, B.M., Goldstein, E.B., De Vries, S., Moore, L.J., Durán Vinent, O., Ruggiero, P., 2019. Exploring marine and aeolian controls on coastal foredune growth using a coupled numerical model. J. Mar. Sci. Eng. 7 (1), 13.

Congalton, R.G., Green, K., 1999. Assessing the Accuracy of Remotely Sensed Data: Principles and Practices. CRC Press.

Dawson, C., Westerink, J.J., Feyen, J.C., Pothina, D., 2006. Continuous, discontinuous and coupled discontinuous–continuous galerkin finite element methods for the shallow water equations. Int. J. Numer. Methods Fluids 52, 63–88.

Dietrich, J.C., Zijlema, M., Westerink, J.J., Holthuijsen, L.H., Dawson, C., Luettich Jr, R.A., ... Stone, G.W., 2011. Modeling hurricane waves and storm surge using integrally-coupled, scalable computations. Coastal Engineering 58 (1), 45–65.

Dolan, R., Lins, H.F., 1985. The Outer Banks of North Carolina. US Government Printing Office.

Doran, K.S., Long, J.W., Overbeck, J.R., 2015. A Method for Determining Average Beach Slope and Beach Slope Variability for US Sandy Coastlines (No. 2015–1053). US Geological Survey.

Durán, O., Moore, L.J., 2013. Vegetation controls on the maximum size of coastal dunes. Proc. Natl. Acad. Sci. 110 (43), 17217–17222.

Elliott, E.A., McKee, B.A., Rodriguez, A.B., 2015. The utility of estuarine settling basins for constructing multi-decadal, high-resolution records of sedimentation. Estuar. Coast. Shelf Sci. 164, 105–114.

Fielding, A.H., Bell, J.F., 1997. A review of methods for the assessment of prediction errors in conservation presence/absence models. Environ. Conserv. 24 (1), 38–49.

Heron Jr., S.D., Moslow, T.F., Berelson, W.M., Herbert, J.R., Steele III, G.A., Susman, K.R., 1984. Holocene sedimentation of a wave-dominated barrier island shoreline: Cape Lookout, North Carolina. Mar. Geol. 60 (1–4), 413–434.

Hesp, P., 1988. Surfzone, beach, and foredune interactions on the Australian South East Coast. J. Coast. Res. 15–25.

Hesp, P., 2002. Foredunes and blowouts: initiation, geomorphology and dynamics. Geomorphology 48 (1–3), 245–268.

Holman, R.A., 1986. Extreme value statistics for wave run-up on a natural beach. Coast. Eng. 9 (6), 527–544.

Jackson, D.W.T., Cooper, J.A.G., del Rio, L., 2005. Geological control of beach morphodynamic state. Mar. Geol. 216, 297–314.

Klemas, V.V., 2015. Coastal and environmental remote sensing from unmanned aerial vehicles: an overview. J. Coast. Res. 31 (5), 1260–1267.

Le Mauff, B., Juigner, M., Ba, A., Robin, M., Launeau, P., Fattal, P., 2018. Coastal monitoring solutions of the geomorphological response of beach-dune systems using multi-temporal LiDAR datasets (Vendée coast, France). Geomorphology 304, 121–140.

Long, J.W., de Bakker, A.T., Plant, N.G., 2014. Scaling coastal dune elevation changes across storm-impact regimes. Geophys. Res. Lett. 41 (8), 2899–2906.

Luettich, R.A., Westerink, J.J., 2004. Formulation and Numerical Implementation of the 2D/3D ADCIRC Finite Element Model Version 44.XX. http://adcirc.org/adcirc_theory_2004_12_08.pdf2004.

Masselink, G., Li, L., 2001. The role of swash infiltration in determining the beachface gradient: a numerical study. Mar. Geol. 176 (2001), 139–156.

Morton, R.A., 2002. Factors controlling storm impacts on coastal barriers and beaches: a preliminary basis for near real-time forecasting. J. Coast. Res. 486–501.

Newe, J., Peters, K., Dette, H.H., 1999. Profile development under storm conditions as a function of the beach face slope. In: Proc. Coastal Sediments '99. ASCE, New York, pp. 2582–2596.

North Carolina Department of Environmental Quality, 2019, July 5. Retrieved from. http://ncdenr.maps.arcgis.com.

Psuty, N.P., 2008. The coastal foredune: A morphological basis for regional coastal dune development. In: Coastal Dunes. Springer, Berlin, Heidelberg, pp. 11–27.

Ranasinghe, R., 2016. Assessing climate change impacts on open sandy coasts: a review. Earth Sci. Rev. 160, 320–332.

Riggs, S.R., Ames, D.V., 2007. Effect of Storms on Barrier Island Dynamics, Core Banks, Cape Lookout National Seashore, North Carolina, 1960–2001 (No. 2006-5309). US Geological Survey.

Rodriguez, A.B., Rodriguez, P.L., Fegley, S.R., 2012. One-year along-beach variation in the maximum depth of erosion resulting from irregular shoreline morphology. Mar. Geol. 291, 12–23.

Rodriguez, A.B., Yu, W., Theuerkauf, E.J., 2018. Abrupt increase in washover deposition along a transgressive barrier island during the late nineteenth century acceleration in sea-level rise. In: Moore, L.J., Murray, B. (Eds.), Barrier Dynamics and Response to Changing Climate. Springer, Cham, pp. 121–145.

Roelvink, D., Reniers, A., Van Dongeren, A.P., de Vries, J.V.T., McCall, R., Lescinski, J., 2009. Modelling storm impacts on beaches, dunes and barrier islands. Coast. Eng. 56 (11 − 12), 1133–1152.

Ruggiero, P., Komar, P.D., McDougal, W.G., Marra, J.J., Beach, R.A., 2001. Wave runup, extreme water levels and the erosion of properties backing beaches. J. Coast. Res. 17, 407–419.

Sallenger, Asbury H. Jr, 2000. Storm Impact Scale for Barrier Islands. J. Coast. Res. 16 (3), 890–895.

Sallenger Jr., A.H., Krabill, W.B., Swift, R.N., Brock, J., List, J., Hansen, M., Holman, R.A., Manizade, S., Sontag, J., Meredith, A., Morgan, K., Yunkel, J.K., Frederick, E.B., Stockdon, H., 2003. Evaluation of airborne topographic lidar for quantifying beach changes. J. Coast. Res. 19, 125–133.

Senechal, N., Coco, G., Bryan, K.R., Holman, R.A., 2011. Wave runup during extreme storm conditions. J. Geophys. Res. Oceans 116 (C7).

Seymour, A.C., Ridge, J.T., Rodriguez, A.B., Newton, E., Dale, J., Johnston, D.W., 2018. Deploying fixed wing Unoccupied Aerial Systems (UAS) for coastal morphology assessment and management. J. Coast. Res. 34 (3), 704–717.

Short, A.D., 1999. Wave-dominated beaches. In: Short, A.D. (Ed.), Handbook of Beach and Shoreface Morphodynamics. John Wiley & Sons, New York, pp. 173–204.

Short, A.D., Hesp, P.A., 1982. Wave, beach and dune interactions in southeastern Australia. Mar. Geol. 48 (3–4), 259–284.

Smith, R.K., Benson, A.P., 2001. Beach profile monitoring: how frequent is sufficient. J. Coast. Res. 573–579.

Stockdon, H.F., Sallenger Jr., A.H., List, J.H., Holman, R.A., 2002. Estimation of shoreline position and change using airborne topographic lidar data. J. Coast. Res. 18, 502–513.

Stockdon, H.F., Holman, R.A., Howd, P.A., Sallenger Jr., A.H., 2006. Empirical parameterization of setup, swash, and runup. Coast. Eng. 53 (7), 573–588.

Stockdon, H.F., Sallenger Jr., A.H., Holman, R.A., Howd, P.A., 2007. A simple model for the spatially-variable coastal response to hurricanes. Mar. Geol. 238 (1–4), 1–20.

Stockdon, H.F., Doran, K.J., Thompson, D.M., Sopkin, K.L., Plant, N.G., 2013. National Assessment of Hurricane-Induced Coastal Erosion Hazards: Southeast Atlantic Coast, USGS Open Report, 2013-1130. https://doi.org/10.3133/ofr20141243.

Susman, K.R., Heron Jr., S.D., 1979. Evolution of a barrier island, Shackleford Banks, Carteret County, North Carolina. Geol. Soc. Am. Bull. 90 (2), 205–215.

Theuerkauf, E.J., Rodriguez, A.B., 2014. Evaluating proxies for estimating subaerial beach volume change across increasing time scales and various morphologies. Earth Surf. Process. Landf. 39 (5), 593–604.

Theuerkauf, E.J., Rodriguez, A.B., 2017. Placing barrier-island transgression in a blue-carbon context. Earth's Future 5, 789–810.
VanDusen, B.M., Theuerkauf, E.J., Fegley, S.R., Rodriguez, A.B., 2016. Monitoring overwash using water-level loggers resolves frequent inundation and run-up events. Geomorphology 254, 32–40.
Wang, P., Briggs, T.M.R., 2015. Storm-Induced morphology changes along barrier islands and poststorm recovery. In: Coastal and Marine Hazards, Risks, and Disasters. Elsevier, pp. 271–306.
Wells, J.T., 1988. Accumulation of fine-grained sediments in a periodically energetic clastic environment, Cape Lookout Bight, North Carolina. J. Sediment. Res. 58 (4), 596–606.
Westerink, J.J., Luettich, R.A., Feyen, J.C., Atkinson, J.H., Dawson, C., Roberts, H.J., et al., 2008. A basin to channel scale unstructured grid hurricane storm surge model applied to southern Louisiana. Mon. Weather Rev. 136 (3), 833–864.
Wright, L.D., 1980. Beach cut in relation to surf zone morphodynamics. In: Coastal Engineering 1980, pp. 978–996.
Wright, L.D., Short, A.D., 1983. Morphodynamics of beaches and surf zones in Australia. In: Komar, P.D. (Ed.), Handbook of Coastal Processes and Erosion. CRC Press, Boca Raton, Florida, pp. 35–64.